JOHNSON MATTHEY
TECHNOLOGY REVIEW

www.technology.matthey.com

Johnson Matthey's international journal of research exploring science and technology in industrial applications

**********Accepted Manuscript**********

This article is an accepted manuscript

It has been peer reviewed and accepted for publication but has not yet been copyedited, house styled, proofread or typeset. The final published version may contain differences as a result of the above procedures

It will be published in the **JULY 2018** issue of the *Johnson Matthey Technology Review*

Please visit the website http://www.technology.matthey.com/ for Open Access to the article and the full issue once published

Note: the doi will not resolve until the final version is published.

Johnson Matthey Technology Review
Johnson Matthey Plc
Orchard Road
Royston
SG8 5HE
UK
Tel +44 (0)1763 253 000
Email tech.review@matthey.com

Accessibility and location of acid sites in zeolites as probed by FTIR and MAS-NMR

Cátia Freitas

Birchall Centre, Keele University, Staffordshire, ST5 5BG, UK

Nathan S. Barrow

Johnson Matthey Technology Centre, Blount's Court, Sonning Common, Reading, RG4 9NH, UK

Vladimir Zholobenko

Birchall Centre, Keele University, Staffordshire, ST5 5BG, UK

Abstract

The understanding of location and accessibility of zeolite acid sites is a key issue in heterogeneous catalysis. This paper provides a brief overview of FTIR and NMR characterisation of acidity in zeolites based on the application of test molecules with a diverse range of basicity and kinetic diameters. A number of zeolites, including ZSM-5 and BEA, have been characterised by monitoring the interaction between the zeolite acid sites and the test molecules, such as 1,3,5-triisopropylbenzene, pyridine and alkylpyridines, to probe the location, accessibility and strength of the Brønsted acid sites. 1,3,5-triisopropylbenzene can be used to distinguish Brønsted acid sites located on the external and internal surface in most medium and large pore channels zeolites. Brønsted acid sites on the external surface of the medium pore zeolites can also be quantified using 2,6-di-ter-butyl-pyridine and 2,4,6-trimethylpyridine. It is concluded that using a combination of probe molecules, including co-adsorption experiments, affords the differentiation between acid sites located in the channels and cavities of different size and on the external and internal surfaces of various zeolitic structures.

https://doi.org/10.1595/205651318X696792

1. Introduction

Zeolites are crystalline solids with a well-defined structure consisting of molecular scale pores and channels. Their primary units such as, SiO_4 and AlO_4 tetrahedra are linked by oxygen atoms at their vertices, creating a variety of microporous framework structures (1). The AlO_4-units impart a negative charge within the framework that must be balanced by cationic species (2). These cationic species are retained by steric effects and electrostatic interactions and can be exchanged with other cations, making zeolites highly valuable as cation-exchangers (2,3,4).

Zeolites have been widely utilized by chemical and petrochemical industries as heterogeneous catalysts. This is due to their unique set of characteristics such as high adsorption capacity, intrinsic acidity, hydrothermal stability and shape selectivity.

Detailed understanding of the acidic properties is important for the design, modification and practical application of zeolite based catalysts. Generally, the most important properties for catalytic reactions are the type, strength, distribution, concentration and accessibility of acid sites. Whilst the microporous nature of zeolites imparts some of their essential properties, such as high surface area, adsorption capacity and shape-selectivity, the presence of micropores can also lead to diffusional limitations, shorter catalyst lifetime and poor activity (5,6)

To achieve full potential of a zeolite catalyst, it is important to maximise the accessibility of active sites and transport efficiency for both the feed molecules and products in catalytic reactions. This can be achieved by employing zeolites with different structures and pore systems, and by introducing mesoporocity in addition to the existing network of micropores. These materials, the so-called hierarchical zeolites, developed, synthesised and modified in numerous ways have received considerable attention (7,8,9,10). The aim of this article is to review recent work evaluating acid site location and accessibility in zeolites with different pore systems, focusing on the understanding of the interactions between acid sites and probe molecules, particularly using FTIR and solid-state NMR, and providing examples of characterisation data for BEA and MFI zeolites using a variety of probe molecules.

2. Location and accessibility of acid sites

The accessibility and location of acid sites in many ways determine the catalytic performance of zeolites. Acid site hosted on the external surface of a zeolite are commonly accessible, the accessibility within the microporous system is dependent upon the dimensions of the pore space relative to the guest molecule. This relationship is closely linked to the local geometry of the acid sites, position of the Al and chemical environment (11,12).

2.1. Infrared spectroscopy

Infrared spectroscopy studies using adsorption of probe molecules is one of the most important tools for comprehensive characterisation, including the nature, strength and accessibility, of acid sites in zeolite based catalysts. The nature and the strength of the Brønsted (i.e. bridging OH-groups) and Lewis acid sites in zeolites has been addressed in detail (11,13,14,15,16,17,18 and references therein); this section is focused on the evaluation of the location and accessibility of acid sites.

Busca and co-authors (19) carried out a range of experiments using pivalonitrile as a probe molecule to distinguish acid sites on internal and external surfaces in MCM-41, FER and MFI type materials (20,21). Other nitriles such as, propionitrile, isobuthyronitrile (22), 2,2-diphenylpropionitrile, benzonitrile and ortho-tolunitrile (23) were also utilised in order to assess the acid site accessibility in a number of zeolitic structures. When compared with other probe molecules, e.g. pyridines and amines, nitriles are interacting with acid sites less strongly, creating a relatively weak bond with the Brønsted and Lewis acid sites (BAS and LAS).

A variety of hydrocarbons have also been used (24); their interaction with acid sites is relatively weak resulting in the formation of a hydrogen bond between the hydrocarbon and a zeolite OH-group. Alkenes and aromatics achieve stronger interactions than saturated hydrocarbons, which are still weak in comparison with other classes of probe molecules. The location and strength of BAS in ZSM-5 zeolites were evaluated by comparing the data obtained for cyclohexane and benzene with those for 1,3,5-trimethylbenzene. It was concluded that the mesoporosity influences only the accessibility of the acid sites by shortening the diffusion pathways, while the strength of the interaction with the probes, reflecting the strength of the acid sites, remains unaffected.

Another approach to understanding the site accessibility in zeolites is co-adsorption of probe molecules with different sizes. Adsorption of a small probe molecule (e.g carbon monoxide) after pre-adsorption of a larger probe molecule was the subject of several studies in mordenite (25,26). This zeolite exhibits two types of channels, 12-membered ring main channels and 8-membered ring channels connected by 8-membered ring side pockets (27). Pyridine can interact with the acid sites in the main channels of MOR but not with those inside the smaller side pockets, whereas CO interacts with all acid sites in the pore system. Consequently, by co-adsorbing these two probes, CO provides information about the strength of Brønsted acid sites in different locations, and the steric hindrance of pyridine gives evidence for the location of the acid sites (26). Co-adsorption of CO and nonane was also used to examine the spatial distribution of platinum in the microspores and mesopores of bi-functional PtH-MFI catalysts (28). This technique involves nonane pre-adsorption between two CO successive chemisorption experiments.

Nesterenko et al. (29,30) and Bleken et al. (31) presented a methodology based on co-adsorption of alkylpyridines and CO for the analysis of acid site distribution in dealuminated mordenites and MFI zeolites. The use of these probe molecules with increasing steric hindrance allows discrimination between acid sites located on the internal and external surface. Both pyridine and alkylpyridines are protonated by BAS. However, due to steric hindrance induced by the bulky substituents, the alkylpyridines probes do not interact with LAS (32). Besides, these bulky probe molecules have limited access to some micropores and consequently are suitable to obtain information about the BAS in different locations (14).

Many reports have been published on the application of 2,6-di-tert-butylpyridine (29,33,34,35) 2,6-dimethylpyridine (29,36,37,38,39) and 2,4,6-trimethylpyridine (30,40,41,42) for zeolite characterisation. For instance, adsorption of pyridine and 2,4,6-trimethylpyridine was used to detect traces of coke in MFI catalysts, and to determine which acid sites are specifically perturbed by coke molecules (43). In the latter study, the authors found that coke deposits, resulting from ortho-xylene isomerisation, do not perturb BAS but perturb non-acidic silanol groups inside the micropore system. Using the same approach, Barbera et al. (41) confirmed that the presence of coke could influence the catalysts deactivation. Both studies clearly distinguish between internal and external silanol groups and show that silanol defects play an important role in the coke formation over MFI catalysts. Corma et al. (34) used the 2,6-di-tert-butylpyridine

to investigate the external surface of a large number of zeolitic structures. 2,6-di-tert-butylpyridine can enter into the 12-membered channels of BEA but not 10-membered ring channels of ZSM-5 and MCM-22. Therefore, it can be used to identify acid sites situated on the external surface of medium pore zeolites.

2,4,6-trimethylpyridine and 2,6-dimethylpyridine were used in a novel approach introduced by Thibault-Starzyk et al. (44), to quantify the accessibility of acid sites in ZSM-5 samples prepared with different degrees of intracrystalline mesoporosity. This approach is based on the calculation of the accessibility index (ACI), the ratio between the number of BAS detected by substituted pyridines and the total number of BAS in the zeolite (detected by Py). The results showed that the formation of mesoporosity reduces the average length of micropores and leads to an increase in the availability of acid sites at the pore mouths. This methodology has been successfully used to evaluate the accessibility of acid sites in both nanocrytalline zeolites and in zeolites with relatively large crystal size (44,45).

Recently, this approach was also applied to other probe molecules, e.g. 2,6-di-tert-butylpyridine was utilised to quantify external BAS in various parent and modified zeolites indicating that the extended mesoporosity and decrease in average length of micropores resulted in the increasing accessibility of BAS (35). Pivalonitrile adsorption was used to quantify both BAS and LAS, including multivalent transition metal cations hosted in zeolites, which are considered as active sites in redox reactions (46).

The quantitative analysis and interpretation of the accessibility studies requires careful consideration. Indeed, the key to quantitative measurements is the use of molar absorption coefficients (ε). For some test molecules, there is a lack of ε values in the literature, and for most, the values reported show a significant degree of variation. Furthermore, the interaction of the probe with the zeolite can be complicated by the pore blockage as some probe molecules can adsorb at the pore mouth of the zeolite and restrict access to the internal pores that once were accessible (47). Also, the strength of interaction with some molecules, such as pyridine and acetonitrile, could lead to "extraction" of the protons from inaccessible positions, making them accessible (48,49). For this reason, some molecules with a relatively large kinetic diameter can access acid sites in small pores of a zeolite. For example, Armaroli et al. (39) reported a different behaviour using probes of similar size (2,6-dimethylpyridine and m-xylene) in ZSM-5. 2,6-dimethylpyridine enters the pores of the ZSM-5 zeolite more readily as compared to

m-xylene. In addition, Traa et al. (50) suggested that the flexibility and the shape of the molecule in relation to the shape of the pore openings should also be taken into account.

Overall, the optimisation of the experimental procedures and the application of a combination of probe molecules are imperative for the successful evaluation of the location and strength of acid sites in different zeolite-based materials.

2.2. MAS-NMR

Both FTIR and ^{1}H NMR can directly probe the acidic proton, which can be used to differentiate BAS and terminal hydroxyls (51). However, the accessibility (location), strength and distribution of acid sites cannot be easily measured by NMR. Basic probe molecules such as pyridine-*d*5 and ^{13}C-acetone have been used to adsorb on the acid sites and reveal their relative strength (52,53). However, ^{1}H has a small chemical shift range giving poor differentiation, and ^{13}C (1.1% naturally abundant) is an insensitive nucleus requiring expensive enriched reagents. Thus, an approach involving ^{31}P was sought, which has both a large chemical shift range and high sensitivity being 100% naturally abundant.

Trimethylphosphine (TMP) was first used in 1985 by Lunsford et al. and has since been used as a probe molecule for BAS and LAS in a variety of solid-acid catalysts (54). TMP can chemisorb on BAS and LAS or physisorb on weakly acidic hydroxyls, each giving a distinct chemical shift range for each type of interaction. Although TMP is a sensitive probe for Lewis acid characterisation, a small Brønsted acid chemical shift range and volatility of the probe molecule has limited the popularity of this approach.

Trimethylphosphine oxide (TMPO), which is a solid at room temperature not susceptible to oxidation, retains the benefits of using ^{31}P NMR and also offers a greater chemical shift range for BAS characterisation. The applicability of TMPO probe molecules was first shown for zeolites by Rakiewicz *et al*. in 1998 (55). Over the past 20 years there have been many ^{31}P NMR studies of phosphorus-containing probe molecules, especially for the industrially-relevant zeolites Beta and ZSM-5 shown in our examples (56,57,58,59,60,61,62,63,64)

A typical procedure for loading a zeolite with TMPO is to first dehydrate the zeolite, then add TMPO dissolved in CH2Cl2 under an inert atmosphere, before heating the sample above the melting point of TMPO (140 °C) (65). However, we and others (66) have also had success in a solvent-free method, by just adding TMPO at elevated

temperatures, which has the added advantage of avoiding any solvent–zeolite interactions. It has been noted that a slight excess of TMPO is crucial in ensuring a complete coverage of acid sites during the experiment (67).

By varying the length of alkyl chain, internal and external acid sites can be discriminated (68). The kinetic diameter of TMPO is 0.55 nm (55), whereas the butyl equivalent, TBPO, is 0.82 nm (69), which is larger than the pore size in ZSM-5.

Unlike TMP, the chemical shift ranges for TMPO interacting with Brønsted and Lewis sites overlap. However, the TMPO adsorption to Lewis sites is weak and it can be readily displaced by water. Thus, acquiring two spectra with and without hydration allows one to determine Brønsted versus Lewis acidity (70).

As NMR is inherently quantitative, by knowing the quantity of TMPO added, a deconvolution of spectral peaks directly gives the concentration of acid sites. Furthermore, the 31P chemical shift of the peaks is linear with Brønsted acid strength (proton affinity), allowing both relative and absolute acid strength to be known (71).

3. Experimental methodology

Ammonium forms of zeolites BEA (CP814E, BEA framework, Si/Al=12.5) and ZSM-5 (CBV8014, MFI framework, Si/Al=40) were obtained from Zeolyst International. Prior to FTIR studies, the zeolites were pressed into self-supporting discs (~8-10 mg) and pretreated *in situ* in an IR cell at 450 °C under vacuum (10^{-5} Torr) for 5 h. The adsorption experiments with different probe molecules were monitored by Thermo iS10 spectrometer equipped with a DSTG detector, at a spectral resolution of 4 cm^{-1}. An excess of probe molecules was admitted by injection of 1.0 µl into the IR cell. Physisorbed molecules were subsequently removed by evacuation at the adsorption temperature. Adsorption of 1,3,5-triisopropylbenzene ($C_{15}H_{24}$, Acros Organics, 95%) was performed at room temperature. Pyridine (C_5H_5N, Acros Organics, 99.5%), 2,6-di-tert-butyl-pyridine ($C_{13}H_{21}N$, Sigma-Aldrich, 97%), 2,6-dimethylpyridine (C_7H_9N, Sigma-Aldrich, 99%) and 2,4,6-trimethylpyridine ($C_8H_{11}N$, BDH reagents, 95%) were adsorbed at 150 °C. Desorption profiles were obtained by evacuating the sample at increasing temperatures in 50 °C steps.

The obtained infrared spectra were analysed (including integration, subtraction, and determination of peak positions) using specialised *Thermo* software, *Omnic*. All the spectra presented in this work were normalized to 10 mg sample mass.

For MAS-NMR experiments, the two zeolite samples were dehydrated at 350 °C under vacuum (10^{-5} Torr) overnight. A slight excess of TMPO was added to the zeolites in an argon glovebox, followed by a treatment at 165 °C for a few hours to melt the TMPO and distribute it throughout the sample. SSNMR spectra were acquired at a static magnetic field strength of 9.4 T on a Bruker Avance III console using TopSpin 3.1 software. A widebore Bruker 4mm BB/1H WVT MAS probe was used, tuned to 161.98 MHz and referenced to ammonium dihydrogen phosphate at 0.9 ppm. The samples were packed into zirconia MAS rotors with Kel-F caps in an argon glovebox.

4. Results and discussion

4.1. Acidity measurements on ZSM-5 and BEA zeolites

MFI structure is characterised by two types of 10-membered ring channels: straight channels with a nearly circular opening of 5.3 Å × 5.6 Å and sinusoidal channels with an elliptical opening of 5.1 Å × 5.5 Å. BEA is a large pore size zeolite with smaller 12-membered ring channels with a cross-section of 5.6 Å × 5.6 Å and larger 12-membered ring channels in with a cross-section of 7.7 Å × 6.6 Å.

FTIR spectra of zeolites BEA and ZSM-5 show two major peaks at 3745 cm-1, with a shoulder at ~3735 cm^{-1}, and 3610 cm^{-1} (Figure 1a). The band at 3610 cm^{-1} is assigned to acidic bridging Si-OH-Al groups and the bands at 3745 and 3735 cm^{-1} are attributed to external and internal silanol groups (Si-OH), respectively. The separation of external and internal silanol groups is more noticeable in the spectra of the BEA zeolite. The interaction of pyridine with ZSM-5 and BEA zeolites results in a complete disappearance of the band at 3610 cm^{-1} corresponding to bridging Si-OH-Al groups and a decrease in the intensity of the band assigned to Si-OH groups. This means that pyridine is able to access all the acid sites of BEA and ZSM-5 providing an overall concentration of acid sites.

In the range of 1400-1700 cm^{-1}, chemisorbed pyridine is revealed by the following sets of bands: 1545 and 1637cm^{-1} is due to pyridinium ion (PyH^+), two bands assigned to Py coordinated to Lewis acid sites (PyL) at 1456 and 1622 cm^{-1} and the superposition of signals of Lewis and Brønsted acid sites at 1491 cm^{-1} (Figure 1b). The concentrations of Brønsted and Lewis acid sites (Figure 2) have been calculated from the intensities of peaks at 1545 cm^{-1} for BAS and 1456 cm^{-1} for LAS. The total concentrations of acid sites for ZSM-5 and BEA parent zeolites are about 350 μmol/g

and 760 μmol/g. ZSM-5 zeolite with Si/Al=40 has less Al in the structure compared to BEA with Si/Al=12.5, and consequently, a lower total concentration of acid sites. The concentration of LAS in ZSM-5 is ~12% of the total number of acid sites. BEA zeolite presents similar amounts of BAS and LAS, 340 μmol/g and 420 μmol/g, respectively. These data are corroborated by ^{27}Al MAS NMR experiments indicating a higher amount of extra-framework aluminium in BEA compared to the ZSM-5 zeolite.

The type and concentration of acid sites can be readily determined from FTIR spectra of pyridine adsorbed on zeolites. Their strength can be evaluated by the temperature programmed desorption of pyridine, ammonia or other probe molecules. However, such measurements give only an effective strength as the probe molecules can re-adsorb on available acid sites during the desorption process. Clearly, the observed apparent strength would be affected by the concentration of acid sites, the size of the micropores as well as by a number of experimental parameters. In contrast, ^{31}P MAS NMR spectra of TMPO-loaded zeolites provide a direct measure of the strength of acid site given by the chemical shift of the phosphorus signal. These data are also quantitative, but they do require complete coverage of the zeolite by TMPO, and therefore, rely on the appropriate dosing procedure being followed.

Figure 3a shows ^{31}P MAS NMR spectra of TMPO dosed ZSM-5 by two different methods, one where TMPO was first dissolved in dichloromethane (DCM) and the other where TMPO was added directly. Both methods produce similar results, whereas the solvent-free method avoids any potential solvent-zeolite interaction. A small excess of physisorbed TMPO is visible around 46 ppm, giving confidence that the accessible acid sites are completely covered. Two types of strong Brønsted site are observed, around 77 ppm and 69 ppm, along with a weaker Brønsted site at 54 ppm. Lewis acid sites from the extra-framework aluminium appeared around 65 ppm. There also appeared to be a very strong Lewis acid site at 84 ppm, but at a very low concentration. The assignment of BAS and LAS has been based on the literature data (70).

Figure 3b presents ^{31}P MAS NMR spectra of TMPO dosed BEA zeolite, obtained via the solvent-free method. A small quantity of mobile TMPO is visible around 31 ppm, suggesting physisorbed TMPO is also present around 46 ppm, but overlapping with Brønsted or Lewis acid sites. Strong BAS can be clearly seen around 75 ppm, along with very strong LAS at 85 ppm. Additional LAS appeared around 65 ppm, as seen for ZSM-5. For BEA, the determination of Lewis versus Brønsted has been based

on hydrating the sample to observe which peaks disappear. The greater quantity of LAS in BEA over ZSM-5 is in agreement with the Py-FTIR and ^{27}Al NMR results.

Further work would be required to obtain accurate data for the concentration of each type of the detected sites. This would involve precise weighing of the samples and TMPO dose that was not undertaken for this study. Additionally, a quantitative analysis of the acid sites present on the internal and external surface could be performed by using bulkier probe molecules such as TBPO.

4.2. Accessibility of acid sites in ZSM-5 and BEA zeolites

Adsorption of 1,3,5-triisopropylbenzene (kinetic diameter of ~8.5 Å) at 30 °C on ZSM-5 and BEA zeolites (Figure 4) leads to a significant reduction in the intensity of the Si-OH band at 3745 cm^{-1}. In the case of BEA (Figure 4c) there is a clear separation between external SiOH groups at ~3745 cm^{-1}, which are interacting with the hydrocarbon molecules, and internal silanols at ~3735 cm^{-1}, which are not. At the same time, the Si-OH-Al band at ~3610 cm^{-1} appears to be almost unchanged. However, the difference spectra (Figures 4b and 4d) show a low intensity negative peak at ~3610 cm^{-1} detected for both zeolites. This negative peak corresponds to the acidic Si-OH-Al groups on the external surface interacting with the probe molecule with the formation of a hydrogen bond. These data demonstrate that 1,3,5-triisopropylbenzene, which is too large to enter the 10- and 12-membered channels of ZSM-5 and BEA, respectively, can be used to quantify the BAS located on the external surface.

FTIR spectra of ZSM-5 zeolite following adsorption of 2,6-dimethylpyridine, 2,4,6-trimethylpyridine and 2,6-di-ter-butyl-pyridine at 250 °C are presented in Figure 5. All the substituted pyridines interact with terminal SiOH groups on the external surface reducing the intensity of the band at 3745 cm^{-1}. The band of Si-OH-Al is virtually unaffected in the case of 2,4,6-trimethylpyridine and 2,6-di-ter-butyl-pyridine adsorption, but does decrease noticeably following adsorption of 2,6-dimethylpyridine indicating that the latter probe can access some of the BAS inside the micropore system. Whereas, 2,6-di-ter-butyl-pyridine and 2,4,6-methylpyridine are not able to enter the micropores of ZSM-5. The difference spectra in the OH region show a low intensity negative peak at ~3610 cm-1 after 2,4,6-trimethylpyridine and 2,6-di-ter-butyl-pyridine adsorption, which corresponds to the small fraction of bridging OH groups located on the external surface of the zeolite or near the pore mouths.

Adsorption of 2,6-dimethylpyridine (Figure 5c, spectrum 1) leads to the appearance of two bands around 1600-1680 cm^{-1} (72). 2,4,6-methylpyridine adsorption (Figure 5c spectrum 2) gives rise to the band at ~1634 with a shoulder at ~1649 cm^{-1} resulting from the interaction with BAS; two low intensity bands at 1619 cm^{-1} and 1575 cm^{-1} are assigned to the probe adsorbed on Si-OH groups (42). The spectra of 2,6-di-ter-butyl-pyridine (Figure 5c spectrum 3) show a band at 1615 cm^{-1} attributed to the probe bonded to BAS (35). Based on the assignment of these bands and the extinction coefficient values available in the literature (30,35,37), the number of BAS accessible to these probe molecules and the corresponding accessibility indices have been calculated assuming 1:1 interaction with the BAS (Table 1). The total amount of BAS is obtained by probing the zeolites with pyridine (44). 2,6-dimethylpyridine being bigger than pyridine, probes 47% of the total amount of BAS, 2,4,6-trimethylpyridine can access 8% and 2,6-di-ter-butyl-pyridine only 5%. These results agree with previously published reports on the adsorption of alkylpyridines on ZSM-5 zeolites (35,44). The diffusion of 2,6-dimethylpyridine, with the kinetic diameter of 6.7 Å, in the micropores of ZSM-5 zeolite (maximum pore size of 5.6 Å) is restricted, depending on the temperature and duration of the experiment it can access up to about 50% of the BAS. These data confirm that the accessibility of the acid sites in the zeolite micropores is controlled by both molecular sieving and strength of interaction between the probe molecule and the acid site. The relatively large size of 2,6-di-ter-butyl-pyridine (7.9 Å) and 2,4,6-trimethylpyridine (7.4 Å) prevents their access to BAS in the micropores of ZSM-5.

In the case of BEA zeolite, the FTIR spectra demonstrate that all three substituted pyridines are protonated on all Si-OH-Al and some Si-OH groups, as they interact with all BAS on the external surface and in the micropores of zeolite BEA. Indeed, the size of the substituted pyridines is similar to the dimensions of the larger pores in the BEA structure (7.7 Å × 6.6 Å) allowing their access to the BAS in the micropore system.

5. Conclusions

Characterisation of the acidic properties of zeolites has received a great deal of attention in the recent decades. FTIR and MAS-NMR are now established as major analytical techniques providing detailed information on the type, concentration, accessibility and location of acid sites. This work demonstrates several examples of FTIR and NMR evaluation of the acidic properties of ZSM-5 and BEA zeolites using a

range of test molecules under in situ conditions. For instance, the accessibility and the number of acid sites on the internal and external surfaces has been determined utilising adsorption of bulky probe molecules monitored by FTIR, hence providing a clear methodology for the detailed examination of the acid sites in MFI and BEA structures. The application of ^{31}P MAS NMR to the analysis of the interactions between TMPO as a probe molecule and the zeolite has provided in-depth information about the type and the strength of the acid sites.

This work can be further extended to include detailed characterisation of new and modified zeolite-based catalysts, particularly, utilising a combination of several techniques. In addition, the experimental methodology should be optimised in order to improve the accuracy of the quantitative analysis under in situ and realistic reaction conditions and for cross-validation of the data obtained from different techniques.

Acknowledgements

We thank Laura Powell for performing initial TMPO experiments as well as Loredana Mantarosie and Markus Knaebbeler-Buss for helping with sample preparation. We gratefully acknowledge Johnson Matthey and Keele University for their support and funding provided for this work.

Table.1. Concentration of Brønsted acid sites and accessibility indices for ZSM-5 zeolite determined using adsorption of alkylpyridines.

	Py	**Lu**	**Coll**	**DTBPy**
Concentration of accessible BAS (µmol/g)	305	143*	25	14
Accessibility index (%)	100	47	8	5

* Depends on the temperature and duration of the adsorption experiment.

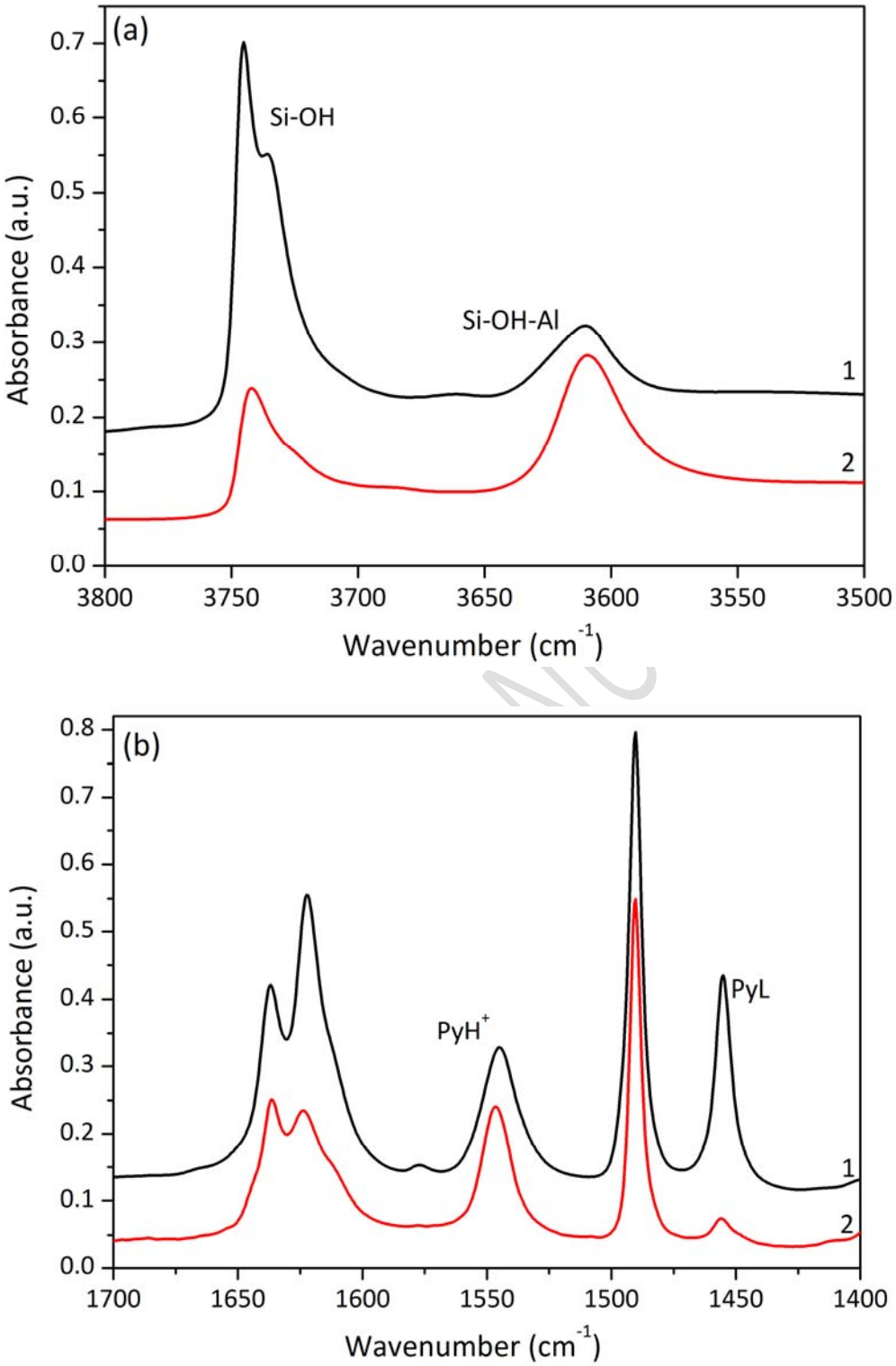

Figure 1. (a) Infrared spectra of the hydroxyl region of BEA (1) and ZSM-5 (2) activated at 450 °C. **(b)** Infrared spectra of the pyridine region folowing pyridine adsorption on BEA (1) and ZSM-5 (2).

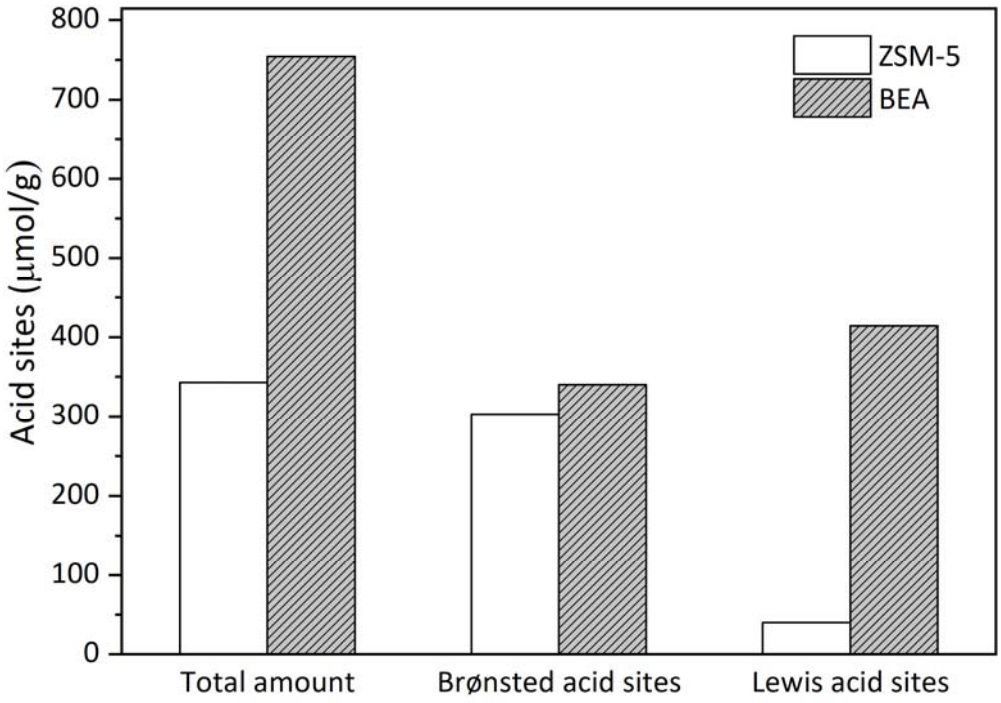

Figure 2. Concentration of acid sites in ZSM-5 and BEA zeolites in quantitative experiments using pyridine adsorption monitored by FTIR.

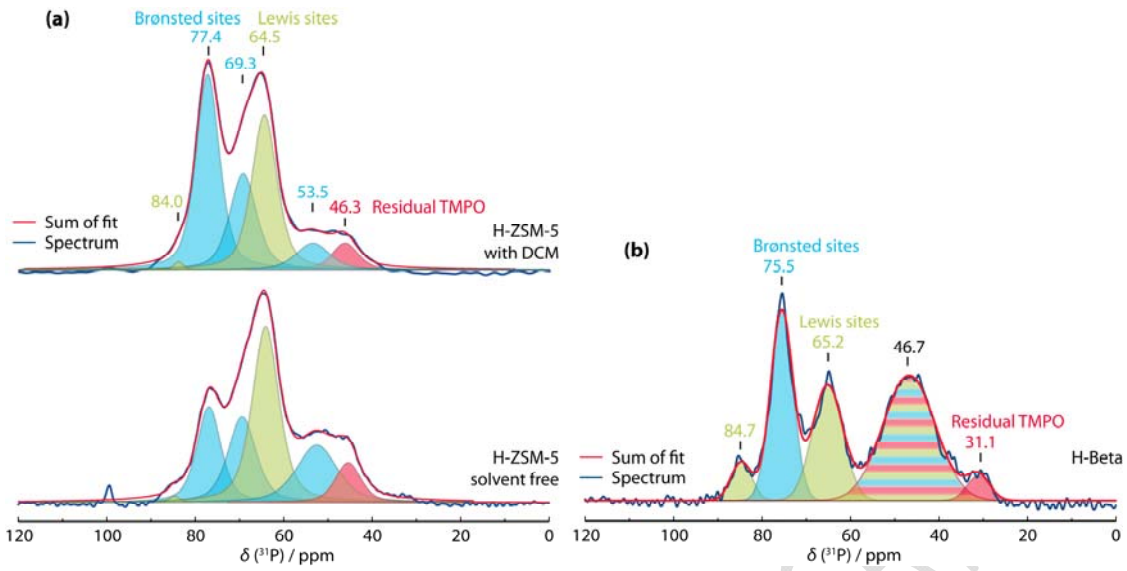

Figure 3. ^{31}P solid-state MAS NMR spectra of (a) ZSM-5 dosed with TMPO, with and without using CH_2Cl_2 as a solvent, (b) BEA dosed with TMPO without solvent.

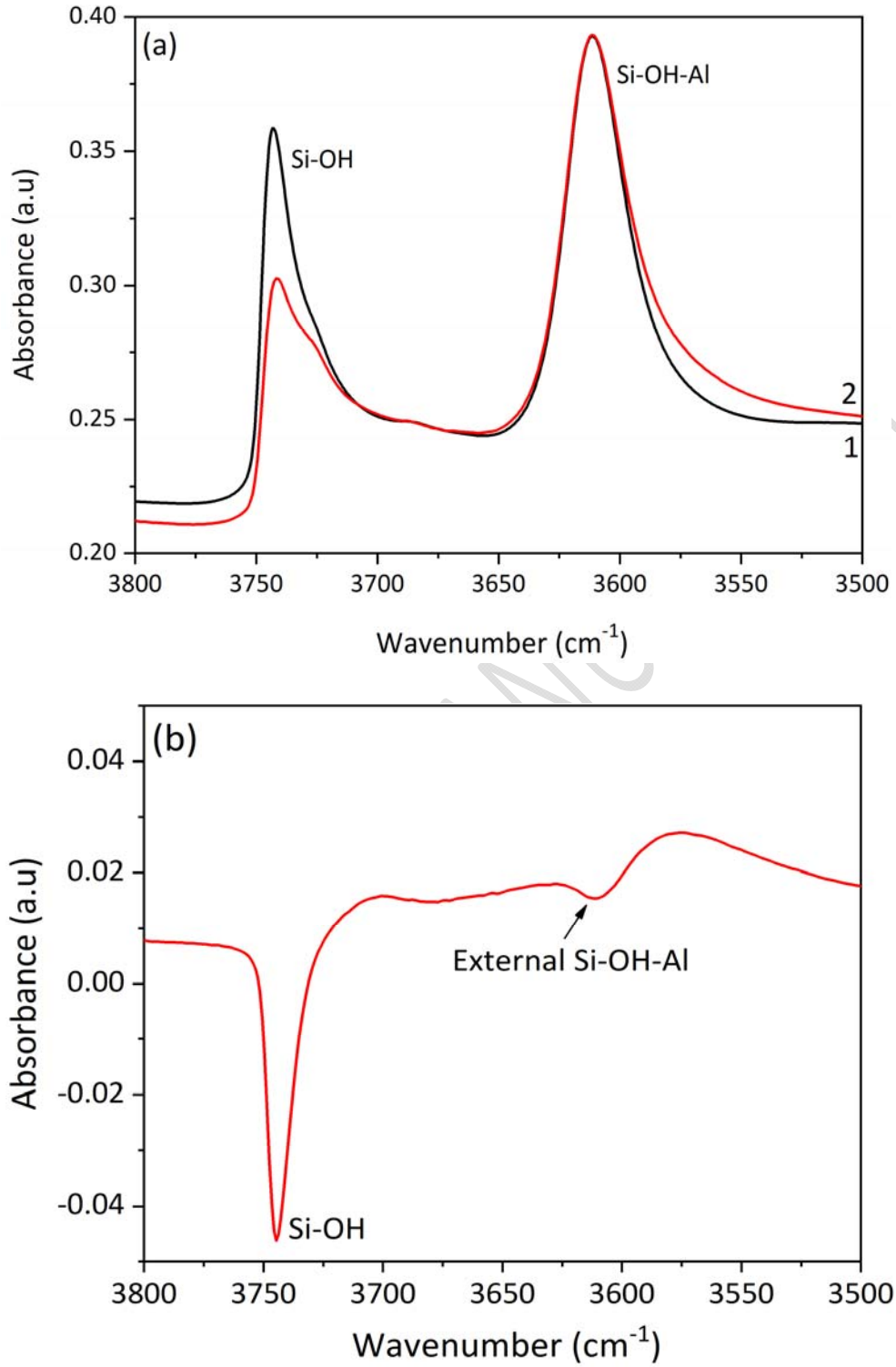
(a)
Si-OH
Si-OH-Al
1
2
Absorbance (a.u)
Wavenumber (cm-1)
(b)
External Si-OH-Al
Si-OH
Absorbance (a.u)
Wavenumber (cm-1)

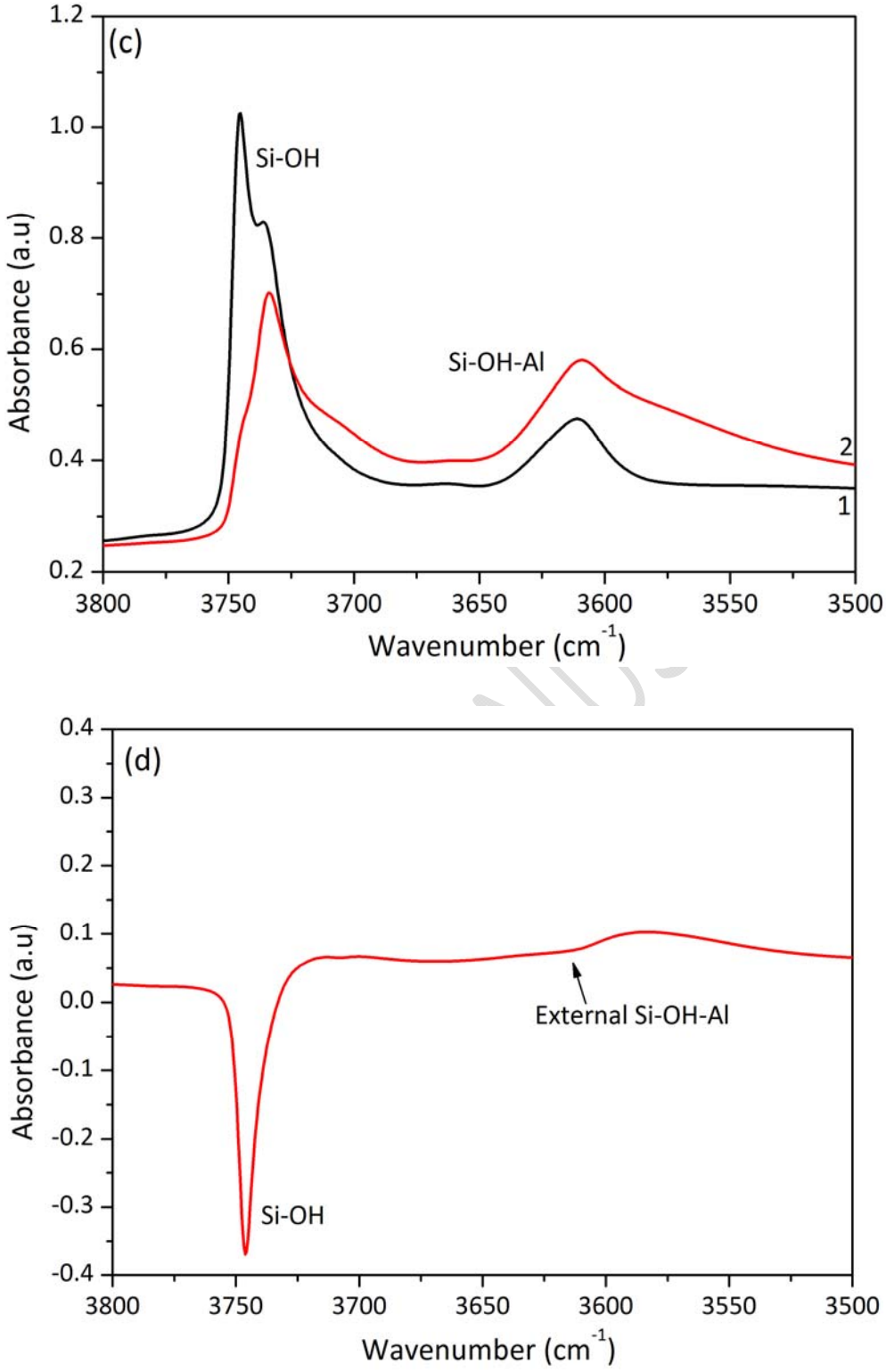

Figure 4. **(a)** FTIR spectra of ZSM-5 before (1) and after (2) 1,3,5-triisopropylbenzene adsorption at 30ºC. **(b)** Difference spectrum of ZSM-5 before and after adsorption of the probe. **(c)** FTIR spectra of BEA before (1) and after (2) 1,3,5-tiisopropylbenzene adsorption at 30ºC. **(d)** Difference spectrum of BEA before and after adsorption of the probe.

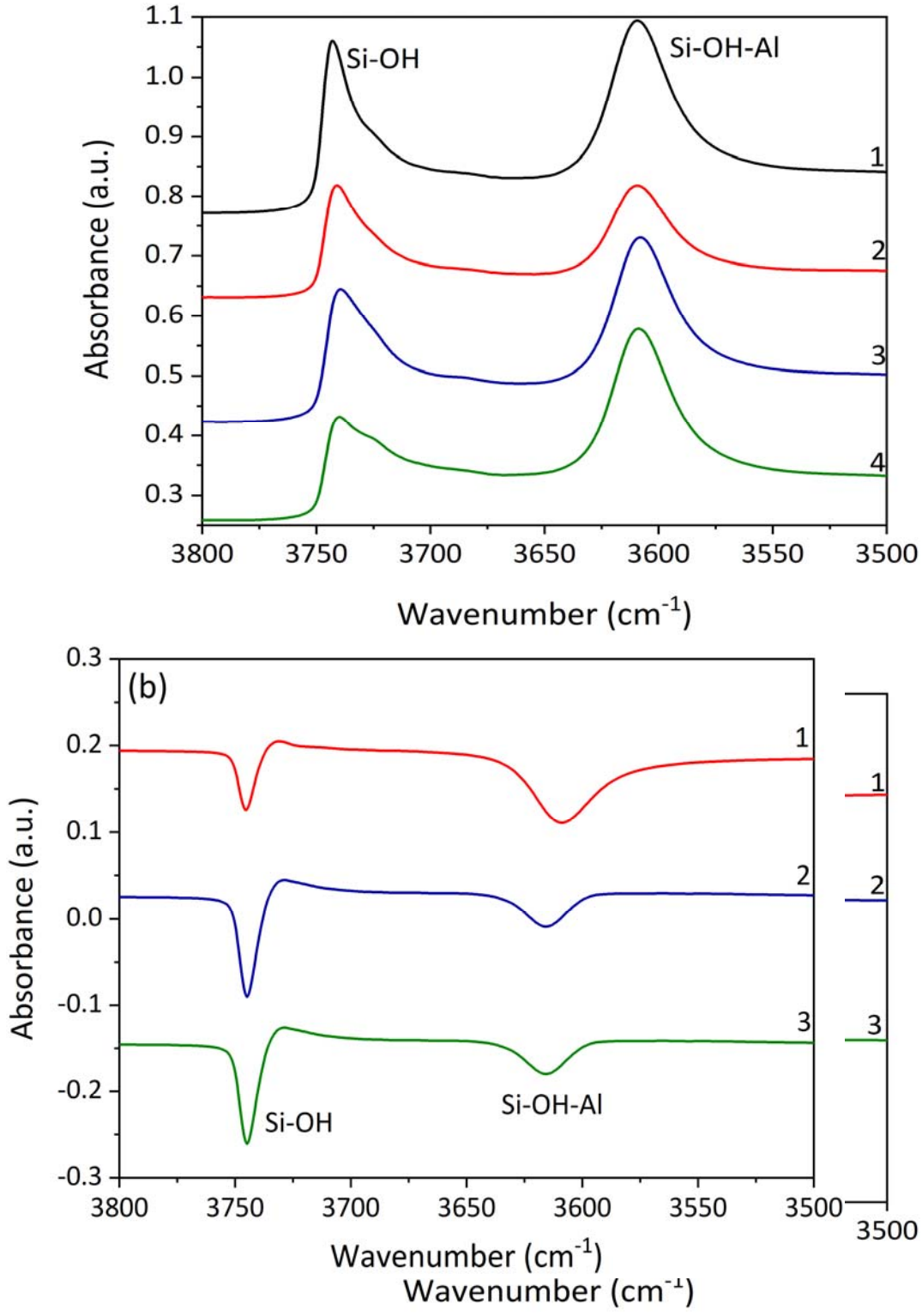
Si-OH
Si-OH-Al
Absorbance (a.u.)
Wavenumber (cm-1)
(b)
Si-OH
Si-OH-Al
Absorbance (a.u.)
Wavenumber (cm-1)
Wavenumber (cm-1)

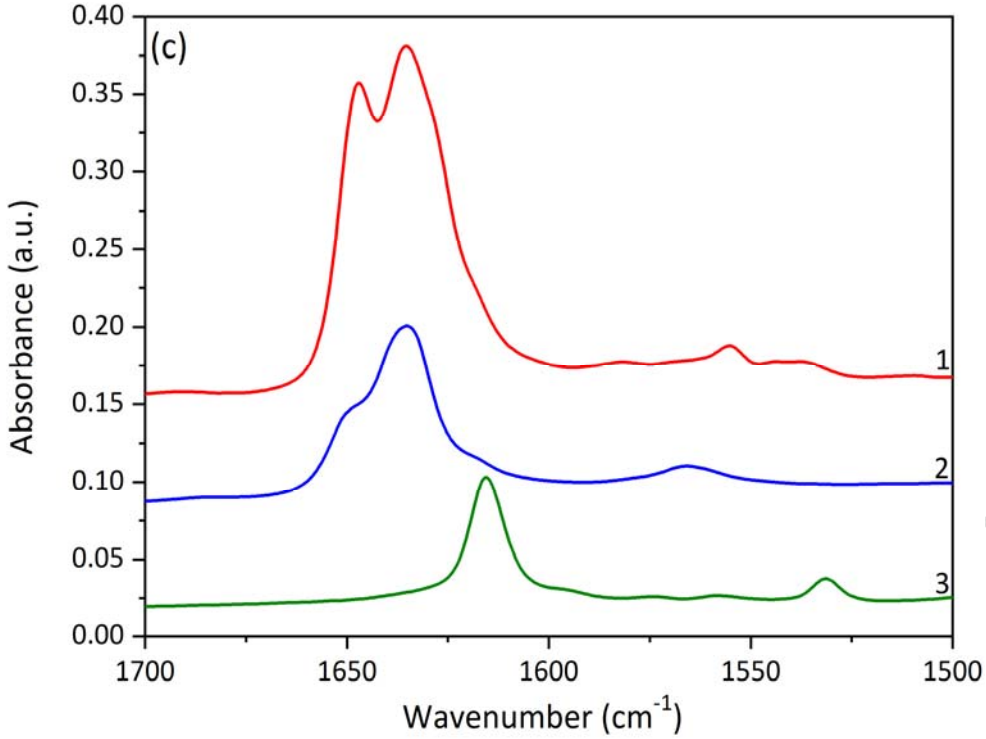

Figure 5. (a) FTIR spectra of ZSM-5 before (1) and after adsorption of alkylpyridines: 2,6-dimethylpyridine (2), 2,4,6-trimethylpyridine (3) and 2,6-di-ter-butyl-pyridine (4). **(b)** Difference spectra in the OH region after adsorptio of alkylpyridines: 2,6-dimethylpyridine (1), 2,4,6-trimethylpyridine (2) and 2,6-di-ter-butyl-pyridine (3). **(c)** Difference spectra in the region of the aromatic ring vibrations of alkylpyridines: 2,6-dimethylpyridine (1), 2,4,6-trimethylpyridine (2) and 2,6-di-ter-butyl-pyridine (3).

Cátia Freitas

Cátia Freitas graduated from the University of Porto, Portugal, in 2012 with a Bachelor's Degree in Chemistry, and a Master's in Chemical Analysis and Characterisation Techniques from the University of Minho, Portugal, in 2014. She worked as a researcher in the Heterogeneous Catalysis and Catalytic Processes (CATHPRO) in Lisbon. Cátia is now in the thied year of a PhD project under the supervision of Dr. Vladimir Zholobenko at the Birchall Centre, Keele University, UK, sponsored by Johnson Matthey. Her research focuses on the FTIR characterisation of acid sites in zeolite-based catalysts in terms of nature, location, concentration and strength.

Nathan Barrow

Nathan Barrow is currently a Principal Scientist in the Advanced Characterisation department at the Johnson Matthey Technology Centre, Sonning Common, UK. He graduated with an MPhys in 2006 from the University of Warwick, UK, where he remained to gain a PhD in SSNMR. In 2010 Barrow was a Knowledge Transfer Partnership associate between the University of Warwick and Johnson Matthey, helping to install and run an SSNMR service. His current research focuses on applying advanced characterisation to materials such as zeolites, alumina, glasses and batteries.

Vladimir Zholobenko

Vladimir Zholobenko is a senior lecturer at Keele University, UK. He graduated with a MSc Diploma in Chemistry from the Moscow State University (USSR), later obtaining his PhD in Chemistry from N. D. Zelinsky Institute of Organic Chemistry (Moscow, USSR). This was followed by postdoctoral research at N. D. Zelinsky Institute of Organic Chemistry, UMIST (Manchester, UK) and Northwestern University (Evanston, US). His current research is concerned with catalysis by zeolites and nanostructured materials and spectroscopic methods of their characterisation.

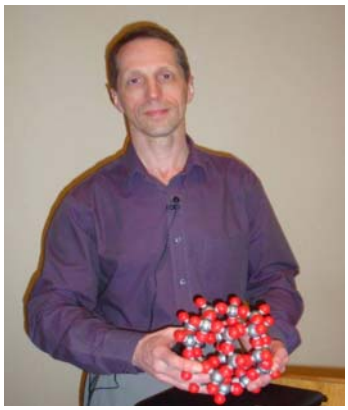

References

(1) J. Weitkamp, *Solid State Ionics*, 2000, 131, (1), 175. Link https://doi.org/10.1016/S0167-2738(00)00632-9

(2) A. Corma, *J. Catal*, 2003, 216, (1-2), 298. Link https://doi.org/10.1016/S0021 9517(02)00132-X

(3) J. Čejka, G. Centi, J. Perez-Pariente and W. J. Roth, *Catal. Today*, 2012, 179, (1), 2. Link https://doi.org/10.1016/j.cattod.2011.10.006

(4) R. Xu, W. Pang and J. Yu, "Chemistry of Zeolites and Related Porous Material – Synthesis and Structure", Q. Huo and J. Chen, John Wiley & Sons, Asia, 2007

(5) A. Corma, *Chem. Rev,* 1997, 97, (6), 2373. Link https://doi.org/10.1021/cr960406n

(6) S. van Donk, A. H. Janssen, J. H. Bitter and K. P. de Jong, *Catal. Rev. Sci. Eng*, 2003, 45, 297. Link http://dx.doi.org/10.1081/CR-120023908

(7) J. Pérez-Ramírez, C.H. Christensen, K. Egeblad, C. H. Christensen and J. C. Groen, *Chem. Soc. Rev,* 2008, 37, (11), 2530. Link http://dx.doi.org/ 10.1039/b809030k

(8)Y. Wei, T. E. Parmentier, K. P. de Jong and J. Zečević, *Chem. Soc. Rev*, 2015, 44, (20), 7234. Link 10.1039/c5cs00155b

(9) M. Milina, S. Mitchell, P. Crivelli, D. Cooke and J. Pérez-Ramírez, *Nat. Commun*, 2014, 5, 1. Link http://dx.doi.org/ 0.1038/ncomms4922

(10) M. E. Davis, "Mesoporous zeolites: preparation, characterization and applications" J. García-Martínez and K. Li, Wiley-VCH Verlag GmbH & Co, Germany, 2015.

(11) K. Hadjiivanov, *Advances in Catalysis*, 2014, 57, 99. Link http://dx.doi.org/10.1016/B978-0-12-800127-1.00002-3

12 D. Zhai, Y. Li, H. Zheng, L. Zhao, J. Gao, C. Xu and B. Shen, *J. Catal,* 2017, 352, 627. Link http://dx.doi.org/10.1016/j.jcat.2017.06.035

(13) C. Lamberti, A. Zecchina, E. Groppo and S. Bordiga, *Chem Soc. Rev*, 2010,39, 4951 Link http://dx.doi.org/ 10.1039/c0cs00117a

(14) S. Bordiga, C. Lamberti, F. Bonino, A. Travert and F. Thibault-Starzyk, *Chem. Soc. Rev.,* 2015, 44, 7262. Link https://doi.org/10.1039/c5cs00396b

(15)A. Vimont, F. Thibault-Starzyk and M. Daturi, *Chem Soc Rev*, 2010, 39, 4928. Link https://doi.org/10.1039/b919543m

(16) M. Niwa, N. Katada and K. Okumura, "Characterisation and Design of Zeolite Catalysis: solid acidity, shape selectivity and loading properties", Springer Science & Business Media, 2010

(17) G. Busca, *Micro. Meso. Mater*, 2017, 254, 3. Link http://dx.doi.org/10.1016/j.micromeso.2017.04.007

(18) L. E. Sandoval-Díaz, J.A, González-Amaya, C. A. Trujillo, *Micro. Meso. Mater*, 2015, 215, 229. Link http://dx.doi.org/10.1016/j.micromeso.2015.04.038

(19) M. Trombetta, G. Busca, M. Lenarda, L. Storaro and M. Pavan, *Appl. Catal, A,* 1999, 182, (2), 225. Link https://doi.org/10.1016/S0926-860X(99)00005-

(20) T. Armaroli, M. Bevilacqua, M. Trombetta, F. Milella, A. G. Alejandre, J. Pérez-Ramírez, B. Notari, R.J. Willey and G. Busca, *Appl. Catal. A*, 2001, 216, (1), 59. Link https://doi.org/10.1016/S0926-860X(01)00543-9

(21) M. Trombetta, T. Armaroli, A. G. Alejandre, J. Pérez-Ramírez and G. Busca, *Appl. Catal. A*, 2000, 192, (1) 125. Link https://doi.org/10.1016/S0926-860X(99)00338-5

(22) M. Bevilacqua and G. Busca, *Catal. Commum,* 2002, 3, (2), 497. Link https://doi.org/10.1016/S1566-7367(02)00196-6

(23) T. Montanari, M. Bevilacqua and G. Busca, *Appl. Catal, A*, 2006, 307, (1), 21. Link https://doi.org/10.1016/j.apcata.2006.03.003

(24) D. Tzoulaki, A. Jentys, J. Pérez-Ramírez, K. Egeblad and J. A. Lercher, *Catal. Today*, 2012, 198, (1), 3. Link https://doi.org/10.1016/j.cattod.2012.03.078

(25) O. Marie, P. Massiani and F. Thibault-Starzyk, *J. Phys. Chem. B*, 2004, 108 (16), 5073. Link https://doi.org/10.1021/jp037915v

(26) M. Maache, A. Janin, J. C. Lavalley, and E. Benazzi, *Zeolites*, 1995, 15, (6), 507. Link https://doi.org/10.1016/0144-2449(95)00019-3

(27) C. Baerlocher, W. H. McCusker, and D. H Olson, "Atlas of zeolite framework types", Elsevier, Amsterdam, The Netherlands, 2001. Link https://doi.org/10.1016/B978-044453064-6/50290-5

(28) L. M. Chua, I. Hitchcock, R. S. Fletcher, E. M Holt, J. Lowe and S.P. Rigby, *J. Catal*, 2012, 286, 260. Link https://doi.org/10.1016/j.jcat.2011.11.012

(29) N. S. Nesterenko, F. Thibault-Starzyk, V. Montouillout, V. V. Yuschenko, C. Fernandez, J. P. Gilson, F. Fajula and I. I. Ivanova, *Micro. Meso. Mater*, 2004, 71, (1-3), 157. Link https://doi.org/10.1016/j.micromeso.2004.03.028

(30) N. S. Nesterenko, F. Thibault-Starzyk, V. Montouilliout, V. V. Yushchenko,C. Fernandez, J. P. Gilson, F. Fajula and I. I. Ivanova, *Kinet. Catal*, 2006, 47, (1), 40. Link https://doi.org/10.1134/S0023158406010071

(31) F. L. Bleken, K. Barbera, F. Bonino, U. Olsbye, K. P. Lillerud, S. Bordiga, P. Beato, T. V. W. Janssens and S. Svelle, *J. Catal*, 2013, 307, 62. Link https://doi.org/10.1016/j.jcat.2013.07.004

(32) P. A. Jacobs and C. F. Heylen, *J. Catal*, 1974, 34, (2), 267. Link https://doi.org/10.1016/0021-9517(74)90036-0

(33) V. V. Ordomsky, V. Y. Murzin, Y. V. Monakhova, Y. V. Zubavichus, E. E. Knyazeva, N. S. Nesterenko and I. I. Ivanova, *Micro. Meso. Mater*, 2007, 105, 101. Link https://doi.org/10.1016/j.micromeso.2007.05.056

(34) A. Corma, V. Fornés, L. Forni, F. Márquez, J. Martínez-Triguero and D. Moscottiy, *J. Catal*, 1998, 179, (2), 451. Link https://doi.org/10.1006/jcat.1998.2233

(35) K. Goìra-Marek, K. Tarach and M. Choi, J. *Phys. Chem. C*, 2014, 118, (23) 12266. Link https://doi.org/10.1021/jp501928k

(36) L. Oliviero, A. Vimont, J. C. Lavalley, F. R. Sarria, M. Gaillard and F. Mauge, *Phys. Chem. Chem. Phy*, 2005, 7, 1861. Link https://doi.org/10.1039/B500689A

(37) T. Onfroy, G. Clet and M. Houalla, *Micro. Meso. Mater,* 2005, 82, (1-2), 99. Link https://doi.org/10.1016/j.micromeso.2005.02.020.

(38) A. Corma, C. Rodellas and V. Fornes, *J. Catal*, 1984, 88, (2), 99. Link https://doi.org/10.1016/j.micromeso.2005.02.020

(39) T. Armaroli, M. Bevilacqua, M. Trombetta, A. G. Alejandre, J. Ramirez and G. Busca, *Appl. Catal. A*, 2001, 220, (1-2), 181. Link https://doi.org/10.1016/S0926-860X(01)00720-7

(40) K. Barbera, F. Bonino, S. Bordiga, T. V. W. Janssens and P. Beato, *J.Catal*, 2011, 280, 195. Link https://doi.org/10.1016/j.jcat.2011.03.016

(41)S. M. T. Almutairi, B. Mezari, E. A. Pidko, P. C. M. M. Magusin and E. J. M. Hensen, *J. Catal*, 2013, 307, 195. Link http://doi.org/10.1016/j.jcat.2013.07.021

(42) M. S. Holm, S. Svelle, F. Joensen, P. Beato, C. H. Christensen, S. Bordiga and M. Bjørgen, *Appl. Catal. A*, 2009, 356, (1), 23. Link https://doi.org/10.1016/j.apcata.2008.11.033

(43) F. Thibault-Starzyk, A. Vimont and J. P. Gilson, *Catal. Today*, 2001, 70, (1-3), 227. Link https://doi.org/10.1016/S0920-5861(01)00420-5

(44) F. Thibault-Starzyk, I. Stan, S. Abello, A. Bonilla, K. Thomas, C. Fernandez, J. P. Gilson and J. Pérez-Ramírez, *J. Catal*, 2009, 264, (1), 11. Link https://doi.org/10.1016/j.jcat.2009.03.006

(45) K. Mlekodaj, K. Tarach, J. Datka, K. Gora-Marek and W. Makowski, *Micro. Meso. Mater*, 2014, 183, 54. Link https://doi.org/10.1016/j.micromeso.2013.08.051

(46) K. Sadowska, K. Goìra-Marek, and J. Datka, *J. Phys. Chem. C*, 2013, 117, (18), 9237. Link https://doi.org/10.1021/jp400400t

(47)A. Zecchina, S. Bordiga, G. Spoto, D. Scarano, G. Spanob and F. Geobaldo, *J. Chem. SOC.,* Faraday *Trans,* 1996, 92, (23), 4863. Link https://doi.org/10.1039/FT9969204863

(48) G. Crépeau, V. Montouillout, A. Vimont, L. Mariey, T. Cseri and F. Mauge, *J. Phys. Chem. B*, 2006, 110, (31), 15172. Link https://doi.org/10.1021/jp062252d

(49) W. Daniell, N. Y. Topsøe and H. Knözinger, *Langmuir* 2001, 17, (20) 6233. Link https://doi.org/10.1021/la010345a

(50) T. Traa, S. Sealy, J. Weitkamp, "Molecular Sieves—Science and Technology", H. G. Karge, J. Weitkamp, Springer-Verlag, Berlin, Heidelberg, 2006. Link https://doi.org/10.1007/3829_003

(51) M. Muller, G. Harvey, R. Prins, *Micro. Meso. Mater*, 2000, 34, (3), 281. Link https://doi.org/10.1016/s1387-1811(99)00180-8

(52) Y. Jiang, J, Huang, W. Dai and M. Hunger, *Solid State Nucl. Magn. Reson*, 2011, 39, (3-4), 116. Link https://doi.org/10.1016/j.ssnmr.2011.03.007

(53)L. E. Sandoval-Díaz, J. A. Gonzalez-Amaya and C. A. Trujillo, *Micro. Meso. Mater*, 2015, 215, (1), 229. Link https://doi.org/10.1016/j.micromeso.2015.04.038

(54) J. H. Lunsford, W. P. Rothwell and W. Shen, *J. Am. Chem. Soc,* 1985, 107, (6), 1540. Link https://doi.org/10.1021/ja00292a015

(55) E. F. Rakiewicz, A. W. Peters and R. F. Wormsbecher, *J. Phys. Chem. B*, 1998, 102, (16), 2890. Link https://doi.org/10.1021/jp980808u

(56) HM. Kao, CY. Yu and MC. Yeh, *Micro. Meso Mater*, 2002, 53, (1-2), 1 Link https://doi.org/10.1016/S1387-1811(02)00279-2

(57). Guan, X. Li, G. Yang, W. Zhang, X. Liu, X. Han and X. Bao, *J. Mol. Catal. A: Chem*, 2009, 310, (1-2), 113. Link https://doi.org/10.1016/j.molcata.2009.06.005

(58) Y. Seo, K. Cho, Y. Jung, and R. Ryoo, ACS Catal., 2013, 3 (4), 713. Link https://doi.org/10.1021/cs300824e

(59) A. Zheng, H.Shing-Jong, W.Qiang, Z.Hailu, D.Feng and L. Shang-Bin, *Chin. J. Catal*, 2013, 34, (3), 436. Link https://doi.org/10.1016/S1872-2067(12)60528-2

(60) A. Zheng, SB. Liu and F. Deng, *Solid State Nucl. Magn. Reson*, 2013, 55-56, 12. Link https://doi.org/10.1016/j.ssnmr.2013.09.001

(61) A. Zheng, F. Deng and S B. Liu, *Annu. Rep. NMR Spectrosc,* 2014, 81, 47. Link https://doi.org/10.1016/B978-0-12-800185-1.00002-4

(62) C. E. Hernandez-Tamargo, A. Roldan and N. H. Leeuw, *J. Phys. Chem. C*, 2016, 120 (34), 19097. Link https://doi.org/ 10.1021/acs.jpcc.6b03448

(63) A. Zheng, S. Li, S B. Liu and F. Deng, *Acc. Chem. Res*, 2016, 49, (4), 655. Link https://doi.org/ 10.1021/acs.accounts.6b00007

(64) R. Zhao, Z. Zhao, S. Li, and W. Zhang, *J. Phys. Chem. Lett*, 2017, 8, (10), 2323. Link https://doi.org/10.1021/acs.jpclett.7b0071

(65)A. Zheng, S. J Huang, S B. Liu and F. Deng, *Phys. Chem. Chem. Phys*, 2011, 13, 14889. Link https://doi.org/10.1039/C1CP20417

(66) S. Hayashi, K. Jimura and N. Kojima, *Micro. Meso. Mater*, 2014, 186, 101. Link https://doi.org/ 10.1016/j.micromeso.2013.11.04

(67) Zheng, S. B Liu and F. Deng, *Chem. Rev*, 2017, 11, (19), 12475. Link https://doi.org/10.1021/acs.chemrev.7b00289

(68) Q. Zhao, W. Chen, S. J. Huang, Y. C. Wu, H. K. Lee and S. B. Liu, *J. Phys. Chem. B*, 2002, 106, (17), 4462. Link https://doi.org/ 10.1021/jp015574k

(69) C. E. Webster, R, S. Drago and M. C. Zerner, *J. Phys. Chem. B*, 1999, 103 (8), 1242. Link https://doi.org/ 10.1021/jp984055n

(70) P. V. Wiper, J. Amelse and L, Mafra, *J. Catal*, 2014, 316, 240. Link https://doi.org/10.1016/j.jcat.2014.05.017

(71) A A. Zheng, L. Chen, J. Yang, M. Zhang, Y. Su, Y. Yue, C. Ye and F. Deng, *J. Phys. Chem. B*, 2005, 109, (51), 24273. Link https://doi.org/10.1021/jp0527249

(72) F. Leydier, C. Chizallet, A. Chaumonnot, M. Digne, E. Soyer, A. A. Quoineaud, D. Costa and P. Raybaud, *J. Catal*, 2011, 284, (2), 215. Link https://doi.org/10.1016/j.jcat.2011.08.015

SUPPLEMENTARY INFORMATION

Accessibility and location of acid sites in zeolites as probed by FTIR and MAS-NMR

Cátia Freitas

Birchall Centre, Keele University, Staffordshire, ST5 5BG, UK

Nathan S. Barrow

Johnson Matthey Technology Centre, Blount's Court, Sonning Common, Reading, RG4 9NH, UK

Vladimir Zholobenko

Birchall Centre, Keele University, Staffordshire, ST5 5BG, UK

Re the data presented in Figure 4, this is an interesting example demonstrating the importance of quantitative data analysis. Although the spectra in Figure 4a appear to coincide around 3600 cm^{-1}, there are important differences, which are shown in Figure 4b in the paper and Figure R1 below. Figure R1 presents the original experimental FTIR spectra of HZSM-5 zeolite, with the green line corresponding to the quantitative subtraction (equivalent to Figure 4b in the paper), which clearly demonstrates the presence of a negative peak attributed to the "removed" bridging OH-groups as they interact with the probe molecule.

The fact that the peak intensities of the red and the blue spectra in Figure R1 are almost the same is explained in Figure R2 presenting the deconvolution of the red spectrum (HZSM-5 after 1,3,5-triisopropylbenzene adsorption). This shows that the red-coloured band at ~3610 cm-1 is a composite of two peaks: one is due to the bridging OH in micropores not interacting with the probe (green-coloured, 3611.7 cm^{-1}), and the second is assigned to the H-bonded SiOH groups interacting with the benzene ring (brown-coloured, 3595 cm^{-1}). The same explanation applies to the spectra obtained for zeolite BEA. These data can be used to quantitatively determine the percentage of the OH-groups on the external surface.

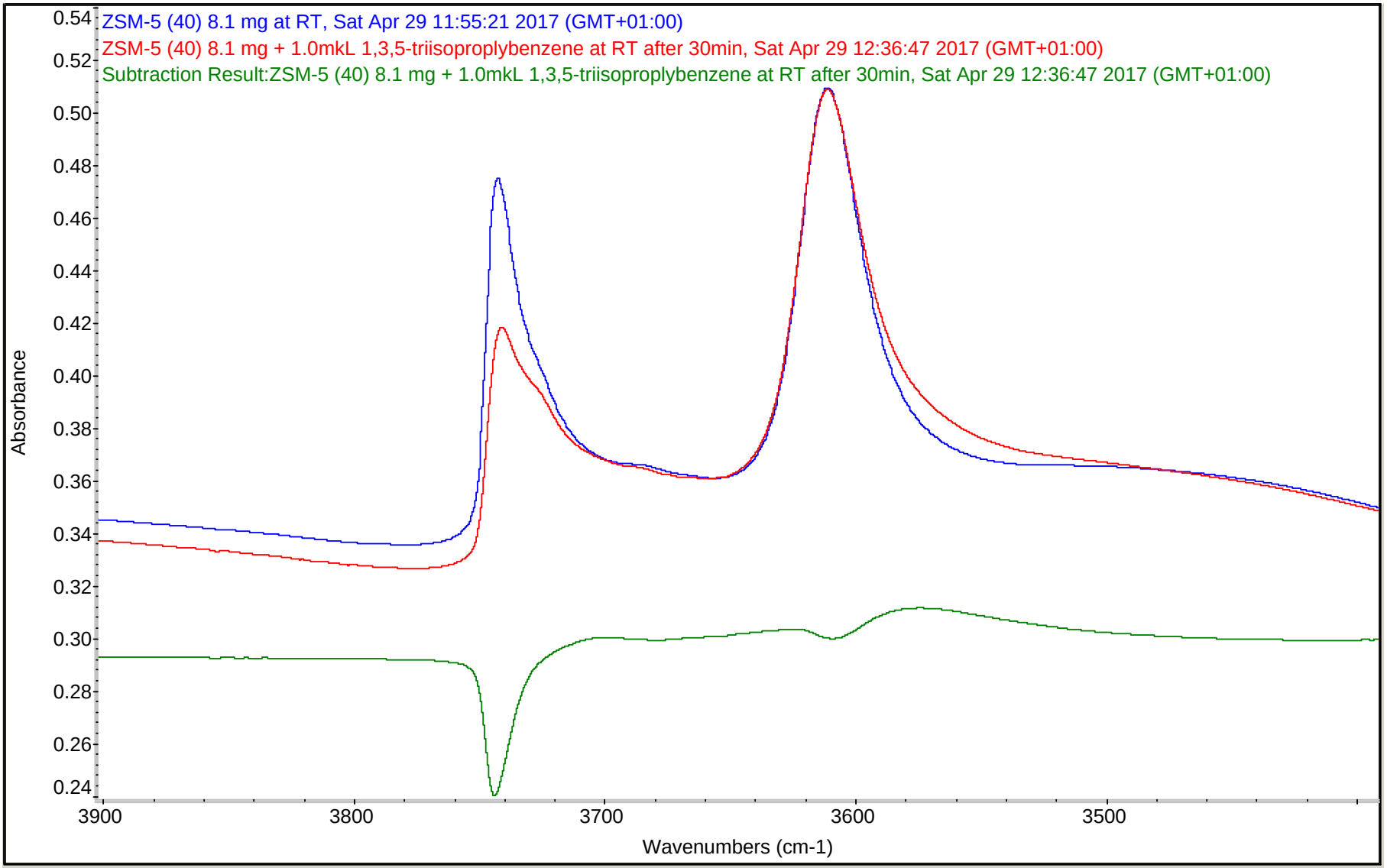

Figure R1. FTIR spectra of ZSM-5 before and after 1,3,5-triisopropylbenzene adsorption at 30°C and the difference spectrum.

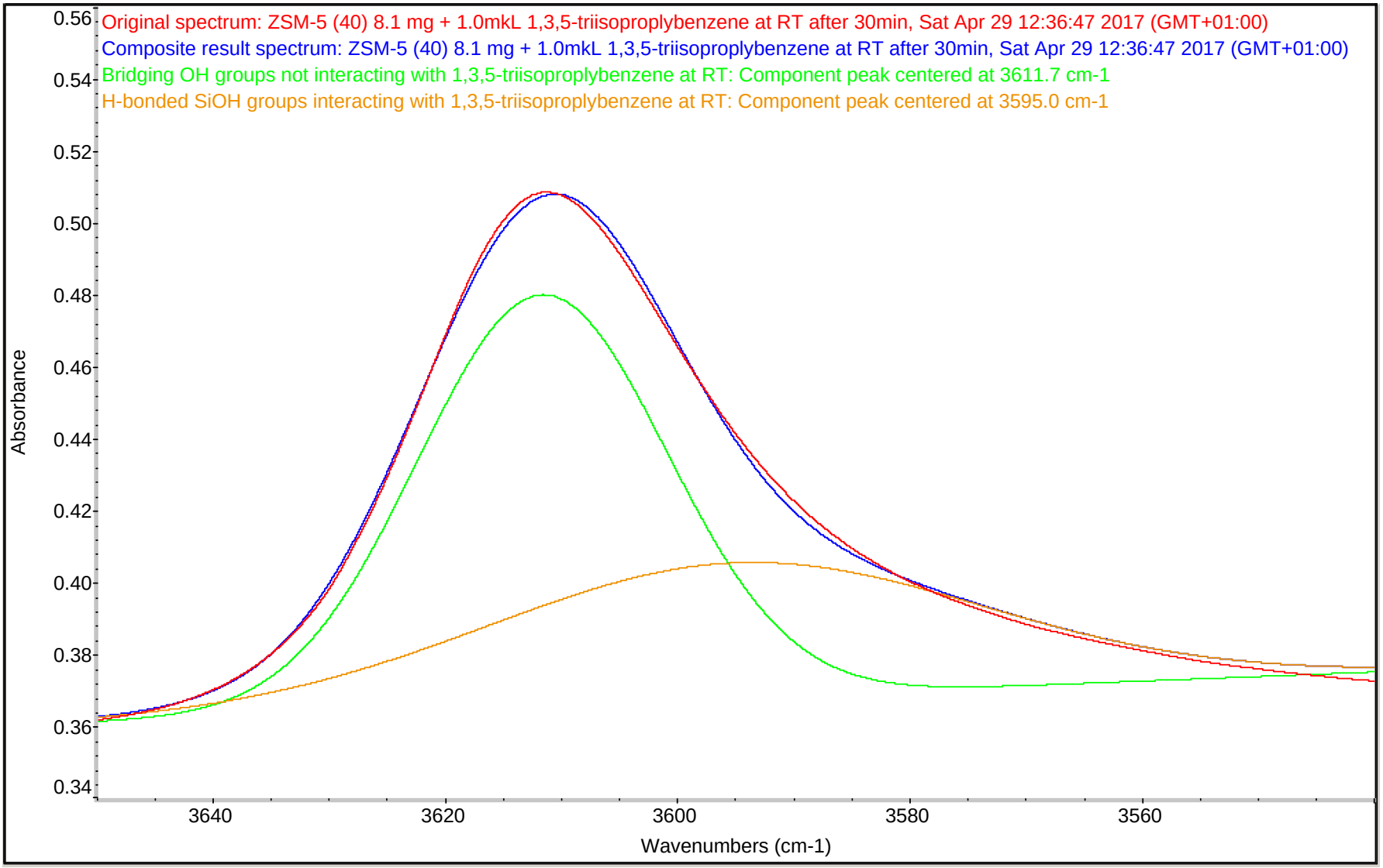

Figure R2. Deconvolution of the FTIR spectrum of ZSM-5 obtained after 1,3,5-triisopropylbenzene adsorption at 30ºC.